

Electric-field-tuned binding energies of trions in silicene, germanene, and stanene monolayers

Roman Ya. Kezerashvili^{1,2}, Shalva M. Tsiklauri,³ and Anastasia Spiridonova¹

¹*New York City College of Technology, The City University of New York, USA*

²*The Graduate School and University Center, The City University of New York, USA*

³*Borough of Manhattan Community College, The City University of New York, USA*

(Dated: August 26, 2024)

We predict the formation of intravalley controllable trions in buckled two-dimensional (2D) materials such as silicene, germanene, and stanene monolayers in an external electric field. Performing a study within the framework of a nonrelativistic potential model using the method of hyperspherical harmonics (HH), the three-body Schrödinger equation is solved with the Rytova-Keldysh potential by expanding the wave functions of a trion in terms of the HH. Then, we numerically solve a resultant system of coupled differential equations. The ground state energies of intravalley trions controlled by the external electric field are presented. The dependencies of the binding energy (BE) of trions in silicene, germanene, and stanene as a function of the electric field are shown to be qualitatively similar. BEs of trions formed by A and B excitons have a non-negligible difference that increases slightly as the electric field increases. We demonstrate that trion BEs can be controlled by the external electric field.

I. INTRODUCTION

The prediction of the existence of trions [1] consisting of an exciton and an electron or a hole, known as negatively or positively charged excitons (X^\mp), gave rise to many theoretical and experimental studies of trions in bulk materials, quantum-well systems, and two-dimensional (2D) materials. Atomically thin transition-metal dichalcogenides (TMDCs) are a class of 2D materials that have remarkable optical and electronic properties [2, 3]. Since the observation of trions in two-dimensional MoS_2 monolayers [4] in 2013, trions have been the subject of intense studies, both experimentally and theoretically, in TMDCs monolayer. In the past decade, different experimental groups have observed and reported the signature of a trion in TMDCs monolayers.

Theoretical studies of trions have integrated a wide variety of techniques and carried them out to calculate the binding energies (BEs) of excitonic complexes in monolayer TMDCs (see the reviews [5–9]). Results for BEs of trions in TMDC monolayers yielded impressively accurate results consistent with experimental data. In the framework of the few-body physics approaches such as the hyperspherical harmonic method and three-body Faddeev equations in configuration or momentum spaces trions in TMDC are investigated in [10–13].

Another category of 2D semiconductors is the buckled 2D allotropes of silicon, germanium, and tin, known as silicene, germanene, and stanene, and collectively referred to as Xenex [14, 15]. Experimental studies revealed one of the most crucial differences between Xenex and graphene and TMDC that Xenex monolayer is not a perfectly flat sheet, but instead it is slightly buckled [14, 16]. As a result, this unique structure of Xenex makes them sensitive to the external electric field applied perpendicular to the monolayer, allowing the band gap to be opened and controlled. The tunable band gap of Xenex gives researchers, among other things, extraordinary in situ control over binding energies and optical properties of excitons in these materials.

In contrast to TMDCs, there is no extensive research on excitonic complexes in Xenex monolayers. The reason is that the synthesis of Xenex monolayers has not been as successful and extensive, as for example, TMDCs monolayers because Xenex monolayers are unstable in the air [17, 18]. In contrast to graphene, silicene and other Xenex monolayers do not occur in nature. Nevertheless, silicene nanoribbons were experimentally synthesized on a metal substrate [19, 20]. This opened the way for silicene, germanene, and stanene monolayers to be transferred on metal such as Au [21–25] and substrates such as MoS_2 , Ir, ZrB_2 [24, 26] and hexagonal boron nitride (hBN) [27, 28] and synthesized as freestanding monolayers [29]. Working with a metallic substrate is easier. For example, silicene grown on Ag (111) [18, 30] and germanene synthesized by dry deposition on Au (111) surface [23] have been thoroughly investigated. However, depositing Xene on a metal leads to a significant alteration of properties of the Xene monolayer. Depending on a substrate, the properties of Xenex monolayers vary; see Refs. [14, 27] for the list of Xenex properties on different substrates. In contrast to deposition on a metal, depositing Xenex on hBN is harder. However, Xene deposited on hBN preserves its properties because Xene and hBN weakly interact [27]. Xenex monolayers deposited on hBN present a particular interest for studying magnetoexcitons in monolayers and vdWHs [31].

Xenex optical and magneto-optical properties have been addressed in Refs. [16, 32–34] and [35, 36], respectively. Different physical phenomena, such as the Hall effect [30], the valley-locked spin-dependent Seebeck effect [37], the anomalous quantum Hall effect [22], the quantum spin Hall effect [38], and the Landau levels [30, 35, 39] are studied

because of their essential role in applications of Xenes monolayers in nanodevices and quantum devices [38, 40–43].

Because of the band inversion, these honeycomb materials are also topological insulators [44–49]. The existence of an excitonic insulator phase in silicene, germanene, and stanene was first studied in [50, 51] in the framework of the effective-mass approximation. The influence of the screening, band dispersion, and external electric field on transitions in Xenes between excitonic, topological, and trivial insulator phases was investigated in [52].

Currently, there is a shortage of research on exciton complexes in Xenes. In particular, there has not been a study of the formation of three quasiparticle states trions in Xenes monolayers. In this paper, we address this gap and focus on a theoretical investigation of trions in Xenes within the method of hyperspherical harmonics (HH).

The paper is organized as follows. In Sec. II, we present nonrelativistic potential model for a system of three interacting electrons and holes, and we employ the three-body Schrödinger equation in the effective-mass approximation. Following [13] in the framework of the HH method, the Schrödinger equation with the Rytova-Keldysh potential [53, 54] is reduced to a system of coupled differential equations for hyperradial functions. A numerical solution of this system provides the BE and wave function for trions in Xenes. In Sec. III, we discuss intravalley X^- and X^+ trions in Xenes monolayers and present results of calculations of controllable ground state energies of intravalley trions by an external electric field. Here, we analyze the dependence of the BEs and a probability distribution of three bound particles on the external electric field. Conclusions follow in Sec. IV.

II. EFFECTIVE-MASS APPROACH FOR TRIONS IN BUCKLED 2D MATERIALS

The starting point of the discussion needs to be the framework of the low-energy model for excitons in Xenes monolayer and heterostructure when the external electric field perpendicular to the structure is present. The detailed overview of the low-energy model for excitons in the buckled 2D material can be found in Refs. [31, 51]. The most stable form of Xenes monolayers has the honeycomb structure where sublattices A and B are offset with respect with each other. The offset is denoted by d_0 and is called the buckling constant. When there is no external electric field, Xenes monolayers resemble graphene in the vicinity of the K/K' points. However, the application of the perpendicular electric field leads to on-site potential difference between sublattices, that results in the variable band gap at the K/K' points that changes electron and hole effective masses. Considering the electric-field-dependent band gap at $p = 0$ [55], the effective mass can be written as:

$$m = \frac{|\xi\sigma\Delta_{gap} - ed_0E_{\perp}|}{v_F^2}, \quad (1)$$

where v_F is the Fermi velocity, $\xi, \sigma = \pm 1$ are the valley and spin indices, respectively, $2\Delta_{gap}$ is the intrinsic band gap, E_{\perp} is the external electric field in z -direction. When $\xi = -\sigma$, the gap is large, since conduction and valence bands are the furthest from the Fermi energy level, and the electron and hole form A excitons. When $\xi = \sigma$, the gap is small and the electron and hole form B exciton. According to Eq. (1) the effective mass of the electron or hole depends on the band gap, Fermi velocity, buckling constant and is a function of E_{\perp} .

The promotion of an electron from the filled valence band to the empty conduction band leaves an empty electron state in the valence band. The description of such a many-body system can be reduced to the two-particle problem of a negatively charged conduction electron interacting with a positively charged valence hole that forms an exciton or other excitonic complexes such as charged excitons or trions. The trions are formed when an exciton binds another electron or hole to form a negatively or positively charged three-particle system: X^- or X^+ , respectively. A description of the properties of trions requires a solution of a three-particle problem. In buckled two-dimensional monolayers, the resulting trions are considered as Wannier-Mott trions since the correlation between an electron and a hole extends over many lattice periods. The representation of the electron-hole pair bound in a Wannier-Mott exciton shows the strong spatial correlation of these two constituents. Therefore, we are assuming that the interaction of the exciton with the third particle (electron or hole) leads to a large-radius-type system.

We follow the approach in which one assumes that the electron and hole bands are isotropic and parabolic, which is a good approximation for the low-energy spectrum of 2D materials. This form of the Hamiltonian implies that both the electron and hole single particle states form a single parabolic band. The corresponding eigenproblem equation reduces to the Schrödinger equation in the effective mass approximation. This approach is commonly used in the literature to describe excitons and trions in 2D materials. See, for example, Refs. [2, 6, 8, 13, 56–60]. Below, we follow the effective-mass approximation.

To obtain the eigenfunctions and eigenenergies of a 2D trion in Xenes when the electric field is perpendicular to the Xenes monolayer, we write the Schrödinger equation for an interacting three-particle electron-hole system. Because we are considering the varying electric field E_{\perp} , which is directed along the z -axis, the corresponding term in the 2D Schrödinger equation vanishes. However, the effect of the electric field action is present through the effective mass as

follows from Eq. (1). Thus, one can write the 2D Schrödinger equation for the interacting three-particle electron-hole system within the effective-mass approximation in the following form

$$\left[-\frac{\hbar^2}{2} \sum_{i=1}^3 \frac{1}{m_i} \nabla_i^2 + \sum_{i<j}^3 V_{ij}(|\mathbf{r}_i - \mathbf{r}_j|) \right] \Psi(\mathbf{r}_1, \mathbf{r}_2, \mathbf{r}_3) = E\Psi(\mathbf{r}_1, \mathbf{r}_2, \mathbf{r}_3), \quad (2)$$

where m_i is the effective mass of the electron or hole defined by Eq. (1), and \mathbf{r}_i is the i th particle position. We assume only two types of charge carriers: an electron and hole with the corresponding effective masses. In Eq. (2), $V_{ij}(|\mathbf{r}_i - \mathbf{r}_j|)$ is the interaction potential between q_i and q_j charges in a 2D material that was first derived in Ref. [53] and was independently obtained by Keldysh [54]. We refer to it as the Rytova-Keldysh (RK) potential. The Rytova-Keldysh potential describes the Coulomb interaction screened by the polarization of the electron orbitals in the 2D lattice and has the following form

$$V_{ij}(r) = \frac{\pi k q_i q_j}{2\kappa \rho_0} \left[H_0\left(\frac{r}{\rho_0}\right) - Y_0\left(\frac{r}{\rho_0}\right) \right], \quad (3)$$

where $r = |\mathbf{r}_i - \mathbf{r}_j|$ is the relative coordinate between two charge carriers q_i and q_j . In Eq. (3) $k = 9 \times 10^9 \text{ N}\cdot\text{m}^2/\text{C}^2$, κ is the dielectric constant of the environment that is defined as $\kappa = (\varepsilon_1 + \varepsilon_2)/2$, where ε_1 and ε_2 are the dielectric constants of two materials that the Xenon layer is surrounded by, ρ_0 is the screening length, which sets the boundary between two different behaviors of the potential due to a nonlocal macroscopic screening, and $H_0(\frac{r}{\rho_0})$ and $Y_0(\frac{r}{\rho_0})$ are the Struve function and Bessel function of the second kind, respectively. The screening length ρ_0 can be written as $\rho_0 = (2\pi\chi_{2D})/(\kappa)$ [56], where χ_{2D} is the 2D polarizability, which in turn is given by $\chi_{2D} = l\varepsilon/4\pi$ [54], where ε is the bulk dielectric constant of the Xenon monolayer. It is worth noting that in Ref. [61] a very good approximation to the RK potential that is simpler to use, fairly precise in both limits, and remarkably accurate for all distances was introduced.

To obtain a solution of the Schrödinger equation (2) for the negatively and positively charged trions, we use the method of hyperspherical harmonics (HH) [62]. The main idea of this method is the expansion of the wave function of the trion in terms of HH that are the eigenfunctions of the angular part of the Laplace operator in the four-dimensional (4D) space. As the first step, let us separate the center-of-mass (c.m.) and the relative motion of three particles and introduce sets of mass-scaled Jacobi coordinates [62, 63]. There are three equivalent sets of Jacobi coordinates and there is the orthogonal transformation between these sets [64, 65]. For three non-identical particles that have different masses the mass-scaled Jacobi coordinates for the partition i read as follows [62–64]:

$$\begin{aligned} \mathbf{x}_i &= \sqrt{\frac{m_j m_k}{(m_j + m_k)\mu}} (\mathbf{r}_j - \mathbf{r}_k), \\ \mathbf{y}_i &= \sqrt{\frac{m_i (m_j + m_k)}{(m_i + m_j + m_k)\mu}} \left(\frac{m_j \mathbf{r}_j + m_k \mathbf{r}_k}{m_j + m_k} - \mathbf{r}_i \right), \quad i \neq j \neq k = 1, 2, 3, \end{aligned} \quad (4)$$

where

$$\mu = \sqrt{\frac{m_i m_j m_k}{m_i + m_j + m_k}} \quad (5)$$

is the three-particle effective mass. In Eqs. (4) the subscripts i , j , and k are a cyclic permutation of the particle numbers.

The transformation (4) allows the separation of c.m. and relative motions of three particles with Hamiltonian (2), and the Schrödinger equation for the relative motion of the three-body system reads

$$\left[-\frac{\hbar^2}{2\mu} (\nabla_{x_i}^2 + \nabla_{y_i}^2) + V(x_1) + V(x_2) + V(x_3) \right] \Psi(\mathbf{x}_i, \mathbf{y}_i) = E\Psi(\mathbf{x}_i, \mathbf{y}_i). \quad (6)$$

In Eq. (6), $V(x_i)$ is the interaction potential between two particles at the relative distance x_1 , x_2 , and x_3 , respectively, where x_i is the modulus of the Jacobi vector \mathbf{x}_i (4), and (6) is written for any of the set $i = 1, 2, 3$ of the Jacobi coordinates (4). The orthogonal transformation between three equivalent sets of the Jacobi coordinates simplifies calculations of matrix elements involving $V(x_i)$ potentials.

This method is presented in detail in Ref. [13] and is briefly outlined here. We introduce in the 4D space the hyperradius $\rho = \sqrt{x_i^2 + y_i^2}$ and a set of three angles $\Omega_i \equiv (\alpha_i, \varphi_{x_i}, \varphi_{y_i})$, where φ_{x_i} and φ_{y_i} are the polar angles for the Jacobi vectors \mathbf{x}_i and \mathbf{y}_j , respectively, and α_i is an angle defined as $x_i = \rho \cos \alpha_i$, $y_i = \rho \sin \alpha_i$. Next, we rewrite the Schrödinger equation (6) for the trion using hyperspherical coordinates in the 4D configuration space [13]. This transformation allows us to reduce the solution of the problem for the three particles in the 2D configuration space to the motion of one particle in the 4D configuration space. Then we introduce the hyperspherical harmonics $\Phi_{K\lambda}(\Omega)$ in the 4D configuration space, which are the eigenfunctions of the angular part of the generalized Laplace operator $\widehat{K}^2(\Omega_i)$ in the 4D configuration space $\widehat{K}^2(\Omega_i)\Phi_{K\lambda}(\Omega) = K(K+2)\Phi_{K\lambda}(\Omega)$ [62], where K is a grand angular momentum. Here we are using the short-hand notation $\lambda \equiv \{l_x, l_y, L, M\}$, where L is the total orbital angular momentum of the trion, M is its projection, and the grand angular momentum $K = 2n + l_x + l_y$, where l_x and l_y are the angular momentum corresponding to \mathbf{x} and \mathbf{y} Jacobi coordinates, respectively, and $n \geq 0$ is an integer number.

The functions $\Phi_{K\lambda}(\Omega)$ present a complete set of orthonormal basis, and one can expand the wave function of the trion $\Psi(\rho, \Omega_i)$ in terms of the HH $\Phi_{K\lambda}(\Omega)$ as

$$\Psi(\rho, \Omega_i) = \rho^{-3/2} \sum_{K\lambda} u_{K\lambda}(\rho) \Phi_{K\lambda}(\Omega_i). \quad (7)$$

In Eq. (7), $u_{K\lambda}(\rho)$ are the hyperradial functions, and by substituting (7) into the Schrödinger equation written in the hyperspherical coordinates [13], one can separate the radial and angular variables and get a set of coupled differential equations for the hyperradial functions $u_{K\lambda}(\rho)$:

$$\left[\frac{d^2}{d\rho^2} - \frac{(K+1)^2 - 1/4}{\rho^2} + \kappa^2 \right] u_{K\lambda}(\rho) = \frac{2\mu}{\hbar^2} \sum_{K'\lambda'} \mathcal{W}_{K\lambda K'\lambda'}(\rho) u_{K'\lambda'}(\rho). \quad (8)$$

In Eq. (8) $\kappa^2 = 2mB/\hbar^2$, where B is trion BE. The coupling effective potential energy $\mathcal{W}_{K\lambda K'\lambda'}(\rho)$ is

$$\mathcal{W}_{K\lambda K'\lambda'}(\rho) = \int \Phi_{K\lambda}^*(\Omega_i) \sum_{i<j}^3 V_{ij}(|\mathbf{r}_i - \mathbf{r}_j|) \Phi_{K'\lambda'}(\Omega_i) d\Omega_i. \quad (9)$$

The coupling effective interaction (9) is defined via the RK potential (3). Substituting (3) into Eq. (9), one obtains the matrix elements of the effective potential energies. The method of calculations of the effective potential energies is given in [13]. Calculations of matrix elements $\mathcal{W}_{K\lambda K'\lambda'}(\rho)$ of the two-body $V_{ij}(|\mathbf{r}_i - \mathbf{r}_j|)$ interactions in the hyperspherical harmonics expansion method for a three-body system are greatly simplified by using the HH basis states appropriate for the partition corresponding to the interacting pair. Using the matrix elements $\mathcal{W}_{K\lambda K'\lambda'}(\rho)$ in Eq. (8), one can solve the system of coupled differential equations numerically. Results of numerical solutions of (9) for trions in Xenes are presented in the next section.

III. INTRAVALLEY TRIONS IN XENES

We apply the present theoretical approach for calculations of the trion BEs in the following freestanding Xenes monolayers: silicene (Si), germanene (Ge), and stanene (Sn) in the external electric field $E_z = E_\perp$ perpendicular to the Xene layer, as shown in Fig. 1. The form of the trion wave function (7) is the most general, not restricted to any particular mass ratio of electrons and holes and describes the three-particle relative motion. The splitting of the conduction and valence bands in Xenes due to spin-orbit coupling at non-zero electric fields leads to the formation of A and B excitons in the larger or smaller band gaps, with corresponding larger or smaller masses of the electron and hole. Two of the three particles constituting a positive or a negative trion in the Xene monolayer have the same masses due to the equity of the mass of electron and hole that form an exciton. However, they are not identical because they have different charges. Below we consider trions formed by a singlet bright A or B exciton and an electron (X^-) or hole (X^+).

In 2D monolayer of Xenes intravalley and intervalley trions can be formed. Here we consider only intravalley trions. An interaction of bright the A or B exciton with another charged carrier in the same valley, which can either be an electron or a hole, forms X^- or X^+ intravalley trion. Schematics in Fig. 2 show the possible formations of the X^- (Figs. 2a and 2b) and X^+ (Figs. 2c and 2d). As follows from Eq. (1), the electron and hole effective masses in A exciton are the same. The B excitons are composed of electron and hole which also have equal masses but smaller than masses of the electron and hole in A excitons. We denoted these masses as m_A and m_B , respectively. The intravalley X^- and X^+ trions have the same two particles' masses. As follows from Eq. (5), the effective masses

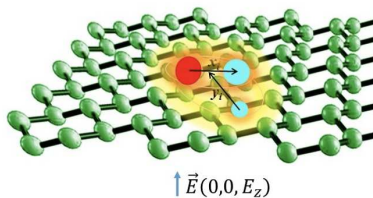


FIG. 1: (Color online) Schematic representation of the X^- trion in the external electric field perpendicular to the freestanding Xenes layer. x_i and y_i are Jacobi coordinates for the partition i .

of the X^- and X^+ trions formed by A or B exciton are $\mu_A = \sqrt{\frac{m_B m_A^2}{m_B + 2m_A}}$ and $\mu_B = \sqrt{\frac{m_A m_B^2}{m_A + 2m_B}}$, respectively [13]. Because $m_A > m_B$, it follows that $\mu_A > \mu_B$. Therefore, the effective mass of the X^- and X^+ trions formed by the A exciton is larger than mass of the X^- and X^+ trions formed by the B exciton. Due to the proportionality of the BE of trions to the three-particle effective mass μ [13], a BE of X^- and X^+ trions formed by the A exciton is larger than BE of trions formed by the B exciton. In the ground state, both intravalley trions formed by charge carriers from the same valley are spin-singlet trions. The intervalley trions can exist in either the singlet or triplet states. They are not considered in this work.

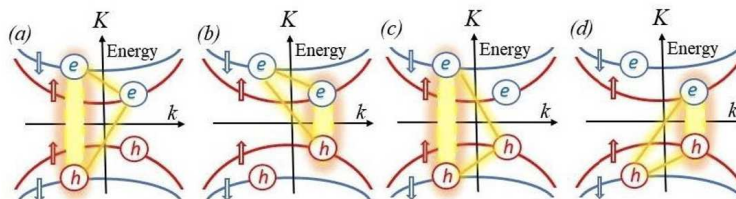


FIG. 2: (Color online) Schematic representation of the low-energy band structure for 2D Xenes material and formation of the intravalley X^- and X^+ trions. Panels (a), (b) and (c), (d) represent the intravalley X^- and X^+ , respectively.

The intravalley X^- and X^+ trions in Xenes monolayers have two particles (the electron and hole) that have the same masses, and the third particle (the electron or hole) has a different mass, as seen in Figs. 2a – 2d. Therefore, we have to deal with three non-identical particles because two particles with the same masses have different charges.

In calculations of the BEs of trions in Xenes monolayers, we use the RK potential. We solve the system of coupled differential equations (8) for the hyperradial functions $u_{K\lambda}^L(\rho)$ numerically. By solving the system of equations (8), one finds the binding energy as well as the corresponding hyperradial functions. The latter allows one to construct the wave function (7). Numerical solution of the coupled differential equations requires the control of the convergence of the BEs for trions with respect to the grand angular momentum K for each value of the external electric field. The relative convergence of the BE is checked as $\Delta B/B = [B(K+2) - B(K)]/B(K)$, where $B(K)$ is the BE for the given K . The analysis of the results for the BEs at different values of the electric field shows that the reasonable convergence is reached for $K_{\max} = 14$, so we limit our considerations to this value.

The input parameters for calculations of BEs of trions in the freestanding are given in Ref. [31]. The formation of Wannier–Mott excitons due to the electron-hole interaction via the RK potential in semiconducting phases in Xenes monolayers occurs when the external electric field exceed some critical value which is unique to each material [50]. A value of the critical electric field is slightly different for A excitons and for B excitons. Following *ab initio* calculations [21] which determined that the crystal structure of silicene becomes unstable around 2.6 V/Å, we consider in our calculations electric fields up to 2.7 V/Å and study the formations of trions in Xenes at the range of the external electric field from the critical value up to 2.7 V/Å. Results of calculations of dependencies of BE of intravalley trions in a singlet state on the external electric field are presented in Fig. 3.

According to Fig. 3, the BE increases for all materials as E_{\perp} increases. In addition, in FS Si, Ge, and Sn, we observe a non-negligible difference in the BE of trions formed by A and B excitons. These differences slightly increase as the electric field increases. The trion BEs for FS Ge and FS Sn are qualitatively similar to FS Si, but they are smaller than freestanding silicene. The curves for FS Ge and Sn qualitatively resemble that of FS silicene, but at 2.7 V/Å FS germanene reaches a maximum trions BE of 24.8 (24.3) meV, and the maximum BE for FS stanene is roughly 21.1 (20.5) meV, significantly smaller than for FS silicene – 30.1 (29.8) meV. In parentheses the BEs of trions formed by B excitons are given. The percent differences between the trion BE of FS Si and FS Ge and FS Si and FS Sn at the largest electric field considered, are 82% (81%) and 70% (69%), respectively.

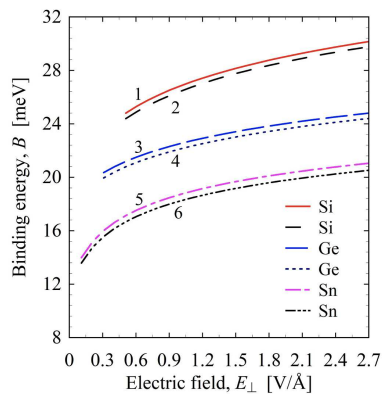


FIG. 3: (Color online) Dependencies of the BE of intravalley triions in freestanding silicene, germanene, and stanene on the applied electric field. Curves 1, 3, and 5 correspond to the triions formed by A excitons coupling an electron (X^-) or hole (X^+), curves 2, 4, and 6 correspond to the triions formed by B excitons coupling an electron (X^-) or hole (X^+). The plots for FS Xenes are truncated for the external electric field E_\perp less than a critical field.

The following conclusions can be made: i. the increase of the BE as the external electric field increases; ii. BEs for FS silicene, germanene, and stanene are qualitatively similar; iii. a non-negligible difference in the BE of triions formed by A and B excitons.

We calculated the probability distribution for the intravalley triion for the spin-valley configuration shown in Fig. 2a. In Fig. 4 the interparticle radial probability distribution for intravalley triions in the silicene monolayer is shown. The difference in the probability distribution is related to the difference of the effective masses μ of intravalley triions. The analysis of the dependence of the probability distribution of three particles on the hyperradius ρ and the external electric field leads to the following conclusion: the increase of the external electric field gives the increase of the triions BE and makes triions more compact since the greater binding energy increases the triion formation probability.

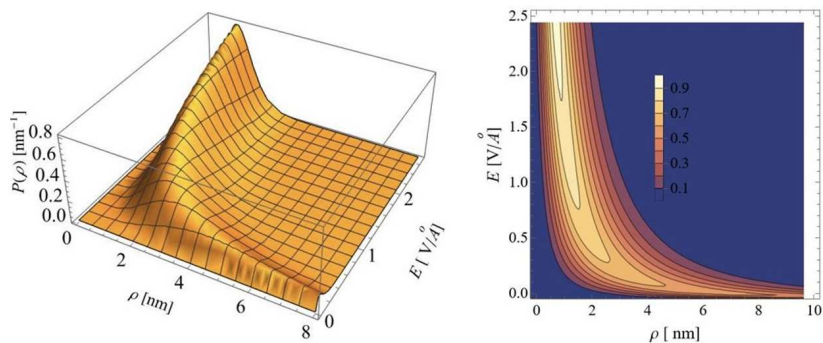


FIG. 4: (Color online) Dependence of the probability distribution of three particles in freestanding silicene on hyperradius ρ and applied electric field for intravalley X^- triion.

IV. CONCLUSION

We predict the existence of electrically controlled triions in Xenes monolayers. We have applied the hyperspherical harmonics method to the calculation of BEs for the triion, and we predict the formation of triions in freestanding Xenes when the external electric field perpendicular to monolayers is present. The results of BEs calculation for triions formed by A and B excitons show a non-negligible difference in triions energies that increases slightly as the electric field increases. The BEs of the intravalley triions can be tuned in the range of 24 – 31 meV for silicene, 21 – 26 meV for germanene, and 14 – 20 meV for stanene by varying the external electric field from the critical value that is specific for each material up to 2.7 V/Å. Let us note that the triion binding energies in Xenes are of the same order as in TMDC monolayers [13]. The dependence of the BE for silicene, germanene, and stanene as a function of the electric field is qualitatively similar. Our findings pave the way toward manipulating the triion BEs by an external electric field. The results of calculations of the probability distribution show an increase in the compactness of triions

with an increase of the electric field, since the greater binding energy increases the trion formation probability.

-
- [1] M. A. Lampert, Mobile and immobile effective-mass-particle complexes in nonmetallic solids, *Phys. Rev. Lett.* **1**, 450 (1958).
- [2] A. Kormányos, G. Burkard, M. Gmitra, J. Fabian, V. Zólyomi, N. D. Drummond, and V. Fal'ko, **k-p** theory for two-dimensional transition metal dichalcogenide semiconductors, *2D Mater.* **2**, 022001 (2015).
- [3] G. Wang, A. Chernikov, M. M. Glazov, T. F. Heinz, X. Marie, T. Amand, B. Urbaszek, Excitons in atomically thin transition metal dichalcogenides, *Rev. Mod. Phys.* **90**, 21001 (2018).
- [4] K. F. Mak, K. He, C. Lee, et al., Tightly bound trion in monolayer MoS₂, *Nat. Mater.* **12**, 207 (2013).
- [5] H. Yu, X. Cui, X. Xu, and W. Yao, Valley excitons in two-dimensional semiconductors, *Natl. Sci. Rev.* **2**, 57 (2015).
- [6] T. C. Berkelbach and D. R. Reichman, Optical and excitonic properties of atomically thin transition-metal dichalcogenides, *Annu. Rev. Condens. Matter Phys.* 2018. **9**, 379–96 (2018).
- [7] M. V. Durnev and M. M. Glazov, Excitons and trions in two-dimensional semiconductors based on transition metal dichalcogenides, *Phys. Usp.* **61**, 825 (2018).
- [8] R. Ya. Kezerashvili, Few-body systems in condensed matter physics, *Few-Body Syst.* **60**, 52 (2019).
- [9] M. A. Semina and R. A. Suris, Localized excitons and trions in semiconductor nanosystems, *Phys. Usp.* **65**, 111 (2022).
- [10] R. Ya. Kezerashvili and Sh. M. Tsiklauri, Trion and biexciton in monolayer transition metal dichalcogenides, *Few-Body Syst.* **58**, 18 (2017).
- [11] I. Filikhin, R. Ya. Kezerashvili, and B. Vlahovic, On binding energy of trions in bulk materials, *Phys. Lett. A* **382**, 787 (2018).
- [12] K. Mohseni, M. R. Hadizadeh, T. Frederico, D. R. da Costa, and A. J. Chaves, Trion clustering structure and BE in two-dimensional semiconductor materials: Faddeev equations approach, *Phys. Rev. B* **107**, 165427 (2023).
- [13] R. Ya. Kezerashvili, S. M. Tsiklauri, and A. Dublin, Trions in two-dimensional monolayers within the hyperspherical harmonics method: application to transition metal dichalcogenides, *Phys. Rev. B* **109**, 085406 (2024).
- [14] A. Molle, J. Goldberger, M. Houssa, Y. Xu, S.-C. Zhang, and D. Akinwande, Buckled two-dimensional Xene sheets, *Nat. Mater.* **16**, 163 (2017).
- [15] J. Zheng, Y. Xiang, C. Li, R. Yuan, F. Chi, and Y. Guo, All-optically controlled topological transistor based on Xenenes, *Phys. Rev. Appl.* **14**, 034027 (2020).
- [16] L. Matthes, O. Pulci, and F. Bechstedt, Massive Dirac quasiparticles in the optical absorbance of graphene, silicene, germanene, and tinene, *J. Phys.: Condens. Matter* **25**, 395305 (2013).
- [17] A. Acun, B. Poelsema, H. J. W. Zandvliet, and R. van Gastel, The instability of silicene on Ag(111), *Appl. Phys. Lett.* **103**, 263119 (2013).
- [18] L. Tao, E. Cinquanta, D. Chiappe, C. Grazianetti, M. Fanciulli, M. Dubey, A. Molle, and D. Akinwande, Silicene field-effect transistors operating at room temperature, *Nat. Nanotechnol.* **10**, 227 (2015).
- [19] B. Aufray, A. Kara, S. Vizzini, H. Oughaddou, C. Léandri, B. Ealet, and G. Le Lay, Graphene-like silicon nanoribbons on Ag(110): A possible formation of silicene, *Appl. Phys. Lett.* **96**, 183102 (2010).
- [20] P. De Padova, C. Quaresima, C. Ottaviani, P. M. Sheverdyaeva, P. Moras, C. Carbone, D. Topwal, B. Olivieri, A. Kara, H. Oughaddou, B. Aufray, and G. Le Lay, Evidence of graphene-like electronic signature in silicene nanoribbons, *Appl. Phys. Lett.* **96**, 261905 (2010).
- [21] N. D. Drummond, V. Zólyomi, and V. I. Fal'ko, Electrically tunable band gap in silicene, *Phys. Rev. B* **85**, 075423 (2012).
- [22] M. Ezawa, Valley-polarized metals and quantum anomalous Hall effect in silicene, *Phys. Rev. Lett.* **109**, 055502 (2012).
- [23] M. E. Dávila, L. Xian, S. Cahangirov, A. Rubio, and G. L. Lay, Germanene: a novel two-dimensional germanium allotrope akin to graphene and silicene, *New J. Phys* **16**, 095002 (2014).
- [24] A. J. Mannix, B. Kiraly, M. C. Hersam, and N. P. Guisinger, Synthesis and chemistry of elemental 2D materials, *Nat. Rev. Chem.* **1**, 0014 (2017).
- [25] C. Grazianetti, C. Martella, and A. Molle, The Xenenes generations: a taxonomy of epitaxial single-element 2D materials, *Phys. Status Solidi RRL* **14**, 1900439 (2020).
- [26] D. Di Sante, X. Wu, M. Fink, W. Hanke, and R. Thomale, Triplet superconductivity in the Dirac semimetal germanene on a substrate, *Phys. Rev. B* **99**, 201106 (2019).
- [27] L. Li, X. Wang, X. Zhao, and M. Zhao, Moiré superstructures of silicene on hexagonal boron nitride: A first-principles study, *Phys. Lett. A* **377**, 2628 (2013).
- [28] A. I. Khan, T. Chakraborty, N. Acharjee, and S. Subrina, Stanene-hexagonal boron nitride heterobilayer: structure and characterization of electronic property, *Sci. Rep.* **7**, 16347 (2017).
- [29] S. Saxena, R. P. Chaudhary, and S. Shukla, Stanene: atomically thick free-standing layer of 2D hexagonal tin, *Sci. Rep.* **6**, 31073 (2016).
- [30] M. Ezawa, Quantum Hall effects in silicene, *J. Phys. Soc. Jpn.* **81**, 064705 (2012).
- [31] R. Ya. Kezerashvili and A. Spiridonova, Effects of parallel electric and magnetic fields on Rydberg excitons in buckled two-dimensional materials, *Phys. Rev. B* **103**, 165410 (2021).
- [32] F. Bechstedt, L. Matthes, P. Gori, and O. Pulci, Infrared absorbance of silicene and germanene, *Appl. Phys. Lett.* **100**, 261906 (2012).

- [33] L. Stille, C. J. Tabert, and E. J. Nicol, Optical signatures of the tunable band gap and valley-spin coupling in silicene, *Phys. Rev. B* **86**, 195405 (2012).
- [34] M. Fadaie, N. Shahtahmassebi, and M. R. Roknabad, Effect of external electric field on the electronic structure and optical properties of stanene, *Opt. Quantum Electron.* **48**, 440 (2016).
- [35] D. Muoi, N. N. Hieu, C. V. Nguyen, B. D. Hoi, H. V. Nguyen, N. D. Hien, N. A. Poklonski, S. S. Kubakaddi, and H. V. Phuc, Magneto-optical absorption in silicene and germanene induced by electric and Zeeman fields, *Phys. Rev. B* **101**, 205408 (2020).
- [36] S. Chowdhury and D. Jana, A theoretical review on electronic, magnetic and optical properties of silicene, *Rep. Prog. Phys.* **79**, 126501 (2016).
- [37] X. Zhai, Y.-T. Wang, R. Wen, S.-X. Wang, Y. Tian, X. Zhou, W. Chen, and Z. Yang, Valley-locked thermospin effect in silicene and germanene with asymmetric magnetic field induced by ferromagnetic proximity effect, *Phys. Rev. B* **97**, 085410 (2018).
- [38] A. Zhao and B. Wang, Two-dimensional graphene-like Xenos as potential topological materials, *APL Mater.* **8**, 030701 (2020).
- [39] V. Y. Tsaran and S. G. Sharapov, Landau levels and magnetic oscillations in gapped Dirac materials with intrinsic Rashba interaction, *Phys. Rev. B* **90**, 205417 (2014).
- [40] C.-H. Chen, W.-W. Li, Y.-M. Chang, C.-Y. Lin, S.-H. Yang, Y. Xu, and Y.-F. Lin, Negative-differential-resistance devices achieved by band-structure engineering in silicene under periodic potentials, *Phys. Rev. Appl.* **10**, 044047 (2018).
- [41] J.-K. Lyu, S.-F. Zhang, C.-W. Zhang, and P.-J. Wang, Stanene: a promising material for new electronic and spintronic applications, *Ann. Phys. (Berlin, Ger.)* **531**, 1900017 (2019).
- [42] N. R. Glavin, R. Rao, V. Varshney, E. Bianco, A. Apte, A. Roy, E. Ringe, and P. M. Ajayan, Emerging applications of elemental 2D materials, *Adv. Mater.* **32**, 1904302 (2020).
- [43] C. Grazianetti, C. Martella, and A. Molle, 8 - Two-dimensional Xenos and their device concepts for future micro- and nanoelectronics and energy applications, edited by L. Tao and D. Akinwande, *Micro and Nano Technologies* (Elsevier, 2020), pp. 181-219.
- [44] F. Bechstedt, P. Gori, and O. Pulci, Beyond graphene: clean, hydrogenated and halogenated silicene, germanene, stanene, and plumbene, *Prog. Surf. Sci.* **96**, 100615 (2021).
- [45] C.-C. Liu, W. Feng, and Y. Yao, Quantum spin Hall effect in silicene and two-dimensional germanium, *Phys. Rev. Lett.* **107**, 076802 (2011).
- [46] M. Ezawa, Monolayer topological insulators: silicene, germanene, and stanene, *J. Phys. Soc. Japan* **84**, 121003 (2015).
- [47] L. Matthes, S. Kűfner, J. Furthműller, and F. Bechstedt, Quantization and topological states in the spin Hall conductivity of low-dimensional systems: An ab initio study, *Phys. Rev. B* **93**, 121106 (2016).
- [48] F. Matusalem, D. S. Koda, F. Bechstedt, M. Marques, and L. K. Teles, Deposition of topological silicene, germanene and stanene on graphene-covered sic substrates, *Sci. Rep.* **7**, 15700 (2017).
- [49] X.-L. Yu, L. Huang, and J. Wu, From a normal insulator to a topological insulator in plumbene, *Phys. Rev. B* **95**, 125113 (2017).
- [50] M. N. Brunetti, O. L. Berman, and R. Ya. Kezerashvili, Can freestanding Xene monolayers behave as excitonic insulators?, *Phys. Lett. A* **383**, 482 (2019).
- [51] M. N. Brunetti, O. L. Berman, and R. Ya. Kezerashvili, Optical properties of excitons in buckled two-dimensional materials in an external electric field, *Phys. Rev. B* **98**, 125406 (2018).
- [52] O. Pulci, P. Gori, D. Grassano, M. D'Alessandro, and F. Bechstedt, Transitions in Xenos between excitonic, topological and trivial insulator phases: influence of screening, band dispersion and external electric field, *SciPost Phys.* **15**, 025 (2023).
- [53] N. S. Rytova, Screened potential of a point charge in a thin film, *Proc. MSU Phys., Astron.* **3**, 30 (1967), https://www.researchgate.net/publication/320224883_Screened_potential_of_a_point_charge_in_a_thin_film.
- [54] L. V. Keldysh, Coulomb interaction in thin semiconductor and semimetal films, *JETP Lett.* **29**, 658 (1979).
- [55] C. J. Tabert and E. J. Nicol, Dynamical polarization function, plasmons, and screening in silicene and other buckled honeycomb lattices, *Phys. Rev. B* **89**, 195410 (2014).
- [56] T. C. Berkelbach, M. S. Hybertsen, and D. R. Reichman, Theory of neutral and charged excitons in monolayer transition metal dichalcogenides, *Phys. Rev. B* **88**, 045318 (2013).
- [57] M. Fogler, L. Butov, and K. Novoselov, High-temperature superfluidity with indirect excitons in van der Waals heterostructures, *Nat. Commun.* **5**, 4555 (2014).
- [58] O. L. Berman and R. Ya. Kezerashvili, High-temperature superfluidity of the two component Bose gas in a transition metal dichalcogenide bilayer, *Phys. Rev. B* **93**, 245410 (2016).
- [59] G. Wang, A. Chernikov, M. M. Glazov, T. F. Heinz, X. Marie, T. Amand, and B. Urbaszek, Colloquium: excitons in atomically thin transition metal dichalcogenides, *Rev. Mod. Phys.* **90**, 021001 (2018).
- [60] O. L. Berman and R. Ya. Kezerashvili, Superfluidity of dipolar excitons in a transition metal dichalcogenide double layer, *Phys. Rev. B* **96**, 094502 (2017).
- [61] P. Cudazzo, I. V. Tokatly, and A. Rubio, Dielectric screening in two-dimensional insulators: implications for excitonic and impurity states in graphane, *Phys. Rev. B* **84**, 085406 (2011).
- [62] J. Avery, *Hyperspherical Harmonics*, Kluwer Academic, Dordrecht, 1989.
- [63] R.I. Jibuti and K. V. Shitikova: *Method of hyperspherical functions in atomic and nuclear physics*, Energoatomizdat, Moscow, 270p. 1993. (in Russian).
- [64] L.D. Faddeev and S.P. Merkuriev, *Quantum scattering theory for several particle systems* (Kluwer Academic, Dordrecht, 1993) pp. 398.

- [65] I. Filikhin, R. Ya. Kezerashvili, and B. Vlahovic, The charge and mass symmetry breaking in the $KK\bar{K}$ system, J. Phys. G: Nucl. Part. Phys. **51**, 035102 (2024).